SLAC-PUB-7349
November 1996

Numerical Modeling of Beam-Environment Interactions in the PEP-II B-Factory[1]

C.-K. Ng, K. Ko, Z. Li and X. E. Lin

Stanford Linear Accelerator Center, Stanford University, Stanford, CA 94309

Invited talk presented at CAP96: Computational Accelerator Physics
Williamsburg, Viginia, Sept. 23-27, 1996.

[1]Work supported by Department of Energy, contract DE-AC03-76SF00515.

SLAC-PUB-7349
November 1996

Numerical Modeling of Beam-Environment Interactions in the PEP-II B-Factory*

C.-K. Ng, K. Ko, Z. Li and X. E. Lin
Stanford Linear Accelerator Center, Stanford University, Stanford, CA 94309

1 Introduction

The PEP-II B-Factory [1] is designed to operate at high currents with many bunches (1658) to achieve the luminosity required for physics studies. Interactions of a beam with its environment in a storage ring raise various issues of concern for accelerator physics, mechanical design and device performance. First, for accelerator physics, wakefields generated by interactions of a beam with beamline components, if not properly controlled, will drive single-bunch and coupled-bunch instabilities [2]. The total broad-band impedance of the ring cannot exceed a budget limited by single-bunch effects. The growth rate of a coupled-bunch mode contributed from narrow-band impedance should be smaller than the damping rate due to synchrotron radiation; otherwise, suppression by feedback control will be necessary. Second, the energy loss by a beam at a beamline component in the form of higher-order-mode (HOM) power leads to additional heating on the component, and to TE mode radiation through openings on vacuum chamber walls. Last, calculations of transfer and beam impedances of pickup and kicker devices are essential for improving their performance and for identifying trapped modes. To address these issues quantitatively requires numerical simulations of each beamline component which include the realistic geometry and the relevant physics involved in the particular beam-environment interactions.

2 Simulations of beam-environment interactions

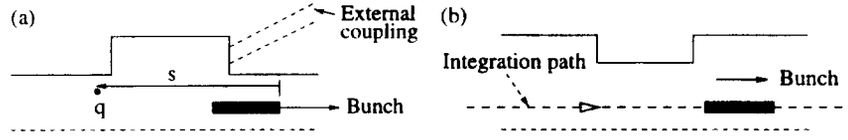

Figure 1: Schematic of beam-environment interaction.

Beam-environment interactions in complex geometries can be studied directly by solving Maxwell equations on a numerical grid in the time domain using a relativistic charged Gaussian bunch. The wakefield generated by the bunch at a beamline component affects particles within the bunch or those in subsequent bunches (see Fig. 1), and its Fourier transform is the impedance. The short-range wakefield corresponds to the broad-band impedance which is governed by excitation above the beampipe cutoff, while the long-range wakefield is associated with the narrow-band resonances below cutoff. The loss parameter, which is the overlap integral of the bunch shape with the short-range wakefield, determines the energy loss.

Many beamline components have external couplings for monitoring or damping purposes. They can be the coaxial cables of a BPM [4] or the damping waveguides of

*Work supported by Department of Energy, contract DE-AC03-76SF00515.

a damped RF cavity [5]. Numerically, these external loading can be represented by ports, and a broad-band matched condition at the ports is required if the response over the frequency range of the beam spectrum is to be evaluated. MAFIA provides this capability so that, for example, one can determine the transfer impedance of the BPM from the beam-induced signal at the coaxial port. Similarly one is able to resolve the external Q's of the HOMs of the damped RF cavity from the long-range wakefield excited by the beam.

There are two methods of wakefield integration in MAFIA. For a cavity-type structure (Fig. 1(a)) where the structure extrudes out of identical upstream and downstream beampipes, one applies the indirect method to integrate the wakefield along the beampipe wall. Then the only contribution comes from integration across the cavity opening. The beampipes can be reasonably short, thus enabling the computations of long-range wakefields. For a collimator-type structure (Fig. 1(b)) where the structure intrudes into the beampipe, one can use the direct method to integrate the wakefield along the bunch path. Now the downstream beampipe has to be sufficiently long in order that the scattered fields off the structure can catch up with the bunch. Specifically the beampipe length L_d has to satisfy $L_d \sim s/(1-v_g/c)$, where s is the distance of the wakefield to be computed and v_g the group velocity of the scattered waves at the bunch r.m.s. frequency. L_d becomes impractically large for short bunches as v_g approaches c and for long-range wakefield calculations for which s is large.

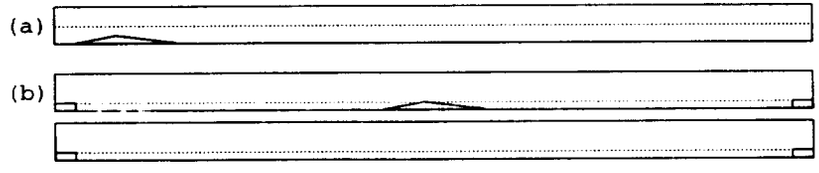

Figure 2: Wakefield calculation of a mask in the vacuum chamber (a) using the direct method; (b) by subtraction of two indirect computations. The dotted lines indicate the integration path in each case.

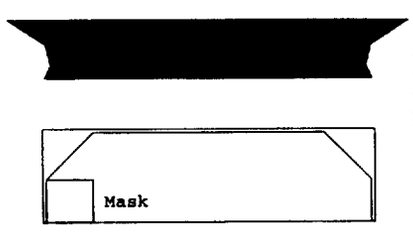

Figure 3: MAFIA model of mask.

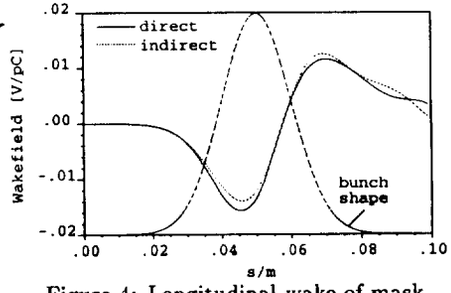

Figure 4: Longitudinal wake of mask.

There is an alternate method to treat collimator-type structures by introducing artificial beampipes at the ends to convert them to cavity-type structures (see Fig. 2(b)). Then the indirect method is applied twice, one with the structure and another without, to obtain the wakefield by subtraction. The error in this method comes from crosstalk between the beampipes and is negligible if they are far apart. We consider a mask in the PEP-II vacuum chamber (see Fig. 3) as an example, and compare the subtraction method with the direct method which requires a long downstream beampipe (Fig. 2(a)). The results from the two methods are shown in Fig. 4. Qualitatively the two wakefields are similar with a difference in the loss parameters of about 15%.

In the following sections we will cover three topics of practical interest related to PEP-II beamline component design that we have investigated with time domain numerical analyses.

3 Beam impedance and transfer impedance

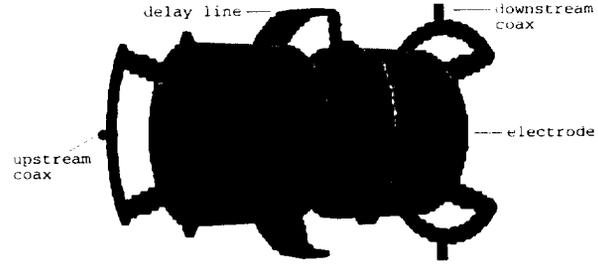

Figure 5: MAFIA model of the longitudinal feedback kicker.

We present the longitudinal feedback kicker as an example of a pickup device. The numerical modeling involves a wakefield analysis in the presence of external couplings. A MAFIA geometry of the device is shown in Fig. 5. The PEP-II kicker has two electrodes in series connected via $\lambda/2$ delay lines to generate voltages across three gaps. It is designed to operate from 952 MHz to 1071 MHz, and to provide a shunt impedance of about 400 Ω over this bandwidth with acceptable beam induced heating of the electrodes. Power in the specified frequency range is driven from a pair of coaxial feeds downstream and couples out at another pair upstream. From the simulation we would like to obtain estimates of the device performance, and to uncover potential danger with trapped modes. We address these issues by calculating the transfer and beam impedances. For numerical expediency (smaller mesh and shorter run time) a 2 cm rather than the actual 1 cm bunch length was used since their spectra differs little over the frequency range of interest. To resolve reasonably well any trapped modes the wakefield was calculated up to 5 m.

Figs. 6(a) and (b) show the monitored signal at the upstream cables and the transfer impedance obtained from its Fourier transform. The transfer impedance $Z_{transfer}$ is fairly constant over the operating bandwidth, and corresponds to a shunt impedance of 353 Ω, using the relationship $R_s = (2Z_{transfer})^2/R_o$ where $R_o = 50\ \Omega$, the coax impedance. This is in good agreement with the measured value of 385 Ω [6]. The longitudinal wakefield and the beam impedance spectrum are shown in Figs. 7(a) and (b). The peak beam impedance around 1 GHz is about 100 Ω which also agrees with measurement. There is a sharp peak at 2.15 GHz with

an impedance of 700 Ω and a Q of 30. This trapped mode has also been observed in measurements [6]. For a total of two kickers in a ring, this HOM contributes 1.4 kΩ which is below the coupled bunch limit of 1.7 kΩ at this frequency. Since Q is low, resonance heating due to coupled bunches is not a concern.

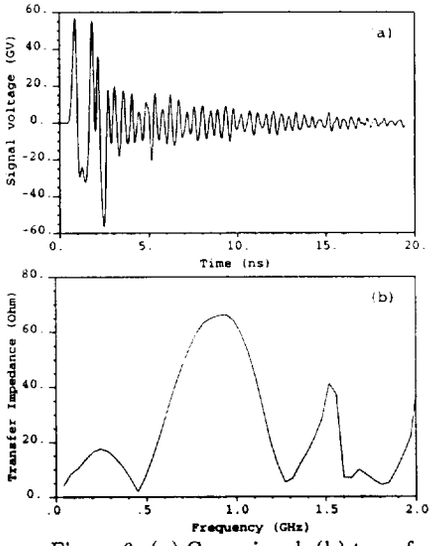

Figure 6: (a) Coax signal; (b) transfer impedance of the kicker.

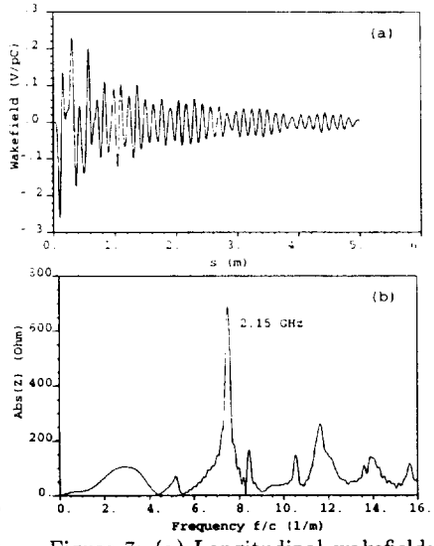

Figure 7: (a) Longitudinal wakefield; (b) beam impedance of the kicker.

4 HOM power dissipation

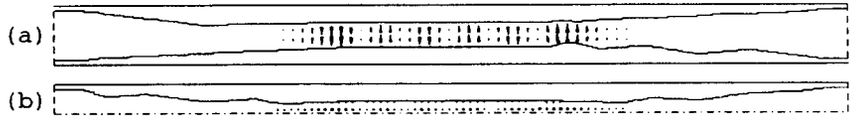

Figure 8: TE_{11} mode trapped in the IR (a) horizontal plane; (b) vertical plane (half of the structure in this plane is shown because of symmetry).

We consider the HOM heating of the beryllium chamber in the interaction region (IR). This central chamber contains the interaction point (IP) and connects at each end to a series of irregularly shaped masks for the purpose of shielding synchrotron radiation before tapering up to larger beampipes at both sides further from the IP. The masks are symmetric with respect to the beam path in the vertical plane but form a constriction at each end of the beryllium chamber (Fig. 8(b)). In the horizontal plane they are not symmetric, which means that the cross section of the vacuum chamber in the mask region varies along the beam path (Fig. 8(a)). The geometry is very large (over 4 m long) and so is the variation in dimension (radius changes from 2 cm to 6 cm over 2 m length). This, and the difficulty to properly terminate the beampipe ends, make mode analysis not a viable approach.

Alternatively we model in the time domain the heating by a single bunch. Instead of the wakefield our focus is on the beam induced currents on the beryllium chamber wall. Fig. 9(a) shows the time variation of the magnetic field at one wall location up to a time of several bunch spacings. The large initial peak is due to the beam image current, and the subsequent oscillations are a result of HOMs. The HOM spectra are shown in Fig. 9(b). The TE_{11} modes are generated because the asymmetry of the masks leads to finite longitudinal electric fields along the beam direction as seen in the mode pattern shown in Fig. 8. This is a 3D effect which previous 2D calculations cannot produce by assuming total symmetry of the masks about the beam axis. It is evident that the HOMs are trapped in the beryllium chamber due to the constrictions in the vertical plane and to mask offsets in the horizontal plane. Using the spectra sampled at many wall locations, one can integrate over the chamber surface to find the power loss. At 3 A current, the wall dissipation is estimated to be 12 W from image current and 2.5 W from HOMs. The enhancement from coupled bunches depends on the loaded Q's of the HOMs, and work is in progress to evaluate this resonant heating to ensure that the cooling specifications can handle the additional dissipation.

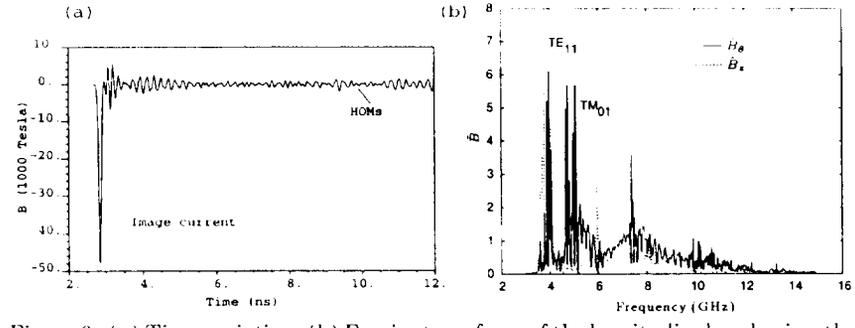

Figure 9: (a) Time variation, (b) Fourier transform of the longitudinal and azimuthal components, of the magnetic field on the beryllium chamber wall.

5 TE power radiation

HOM TE power will propagate in the PEP-II rings after being generated by the beam at asymmetric beamline components such as the RF cavities. The concern is that this power may have adverse effects on a beamline component and its surroundings if it is allowed to radiate through openings in the vaccum chamber wall. An example is the distributed-ion-pump (DIP) screen employed to separate the pump chamber from the beam chamber. The screen is primarily designed to provide adequate conductance for pumping not at the expense of generating high beam impedance. Now additional consideration to prevent TE power radiation from damaging the pumps in the pump chamber has to be included.

MAFIA models of a design with 4-cm slots and a 'microwave screen' design consisting of 3mm×3mm holes are shown in Fig. 10. We compare their effectiveness in screening out TE power by a transmission calculation of a TE_{10} mode propagating in the beam chamber. The results are shown in Fig. 11. The deviation of the

transmission coefficient from unity represents radiation through openings on the chamber wall. The slotted design is found to allow non-negligible penetration over a broad range of frequencies, especially around 3.3 GHz. Apparently, the slots are long enough to interrupt the azimuthal current of the TE mode. In contrast, the screen design is basically opaque to TE penetration at all frequencies with 100% transmission. In light of this comparison, the final design consists of six continuous grooves of 5.64 m long and 3.75 mm wide, with round holes of diameter 3 mm hidden halfway inside. The broad-band impedance of this hidden hole design is extremely small and has been described in Ref. [7].

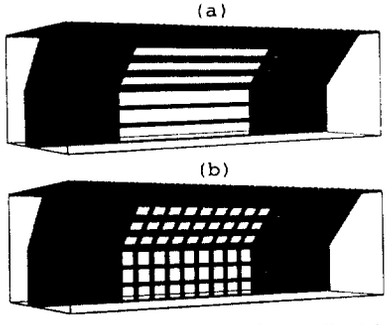

Figure 10: Vacuum chamber wall with (a) slots; (b) a screen. Only parts of the models of the beam and pump chambers are shown.

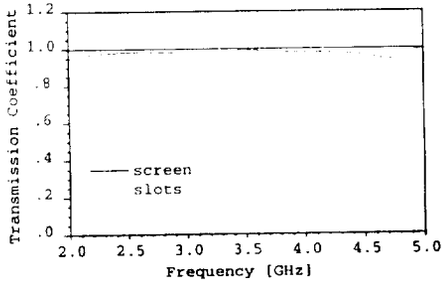

Figure 11: Transmission coefficients of TE_{10} mode for the slots and screen.

6 Summary

For the past three years, we have modeled many of the PEP-II beamline components and have helped optimize their designs to meet the requirements of beam impedance, mechanical design or device performance. We have tried to benchmark our simulation models with measured data whenever they are available. The methodology described here can be applied to other storage rings such as light sources and the damping rings in linear colliders.

Acknowledgements

We are grateful to many members of the PEP-II collaboration at SLAC, LBNL and LLNL for their collaboration on modeling the PEP-II beamline components. We thank Sam Heifets for theoretical discussions, and Thomas Weiland and Martin Dohlus for their expertise with MAFIA.

References

[1] An Asymmetric B Factory, Conceptual Design Report, SLAC-418, June 1993.
[2] S. Heifets et. al., Impedance Study for the PEP-II B-Factory, SLAC-PUB-6989, 1996.
[3] MAFIA User's guide Version 3.20, CST GmbH, Darmstadt, Germany.
[4] N. Kurita et. al., Numerical Simulation of the PEP-II Beam Position Monitor, SLAC-PUB-7006, 1995.
[5] E. Lin, K. Ko and C. Ng, Impedance Spectrum for the PEP-II RF Cavity, SLAC-PUB-6902, 1995.
[6] J. Corlett and J. Byrd, PEP-II Longitudinal Feedback Kickers- Prototype Measurement Results, 1996.
[7] C.-K. Ng and T. Weiland, Impedance of the PEP-II DIP Screen, SLAC-PUB-7005 1995.